Processor In the Loop implementation of two stages Backstepping control strategy for Permanent Magnet Synchronous Motor based load torque observer

Mohammed El Haissouf[1*], *Mustapha* El Haroussi[1], *Abdellfattah* Ba-Razzouk[1], and *Mounir* Bensaid[1]

[1]Department of Applied Physics, MISI Laboratory, FST, University Hassan 1st, Settat, Morocco

Abstract. This work deals with Backstepping control strategy for permanent magnet synchronous motor drive, using load torque observer. The proposed study uses a modified motor model with new variables, dynamic separation and Luenberger load torque observer. This paper proposes a precise calculation method for controller and observer parameters based on response time and damping coefficient. Validation is performed using Processor In the Loop technique and code generation from Simulink. Results show that Backstepping works well by adding disturbance observer so accuracy is ensured. In addition, response time is respected due to the precise controller design.

Keywords: Nonlinear control strategy, Backstepping, Permanent Magnet Synchronous Motor, Load torque estimation, Luenberger observer, Processor In the Loop technique.

1 Introduction

In this paper, we propose synthesizing a Backstepping control [1] [2], with a load torque observer, for a synchronous motor with dynamic separation where the current loop is faster than the speed loop [3][4]. In this work the inner loop is ten time faster than the outer loop. Fig. 1 shows a synoptic diagram of the proposed control, highlighting the main algorithm separated on two steps, the load torque observer, the $Park$ transformation and the SVM generator [5][6].

The control system consists of two blocks: a first block ensures speed control and generates the current reference values, while the second block ensures the current control and generates the control law signals [7]. The direct current reference can be overridden, but there are other criteria for calculating current references, such as minimizing the current modulus [8].

The proposed control strategy is designed to ensure a precise dynamic $trv = 100\,ms$ with no override, a good accuracy and a negligible current distortion. So we give more interest to the parameters calculation as well as the SVM frequency in comparison to similar studies.

Proposed validation method is based on PIL technique. So the motor model is implemented on $Simulink$ as well as the inverter's one and the control algorithm runs on an actual DSP, while the communication between the controller and the plant is ensured by a serial link via USB ports.

NB: Nomenclature is given at the end of the paper.

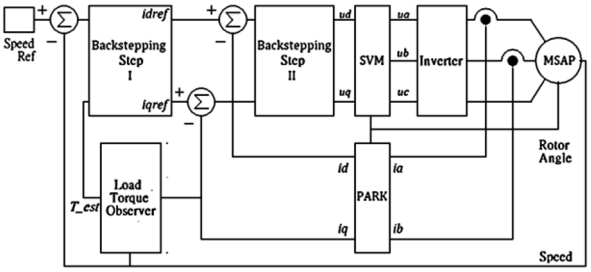

Fig. 1. Backstepping diagram of PMSM control

2 State space model of the PMSM

This is a nonlinear third-order system with coupled variables [9]. The mechanical equation may be separated from the electrical equation, but it is possible to integrate them in the same matrix expression, as in the following equation (1). It is a non-linear, coupled, multi-input, multi-output system [10].

$$\frac{d}{dt}\begin{bmatrix}\Omega\\ i_d\\ i_q\end{bmatrix}=\begin{bmatrix}-\frac{1}{Tm}\Omega+\frac{3p}{2J}\left(\varphi_M i_q+\left(L_d-L_q\right)i_d i_q\right)-\frac{C_R}{J}\\ -\frac{1}{Td}i_d+p\Omega\frac{L_q}{L_d}i_q\\ -\frac{1}{Tq}i_q-p\Omega\frac{L_d}{L_q}i_d-p\Omega\varphi_M\frac{1}{L_q}\end{bmatrix}+\begin{bmatrix}0 & 0\\ \frac{1}{L_d} & 0\\ 0 & \frac{1}{L_q}\end{bmatrix}\left[v_{dq}\right] \quad (1)$$

* Corresponding author: elhaissouf@gmail.com

3 Model of the SVM inverter

SVM technique is based on the comparison of three reference signals ua, ub, uc, forming a balanced three-phase system, with a triangular signal uo of high frequency carrier [11][12].

The signals resulting from this comparison are thus pulse-width modulated sequences at the same rate as the control signals.

Hence the relationship between inverter output voltages and control signals is expressed in equation (2).

$$\begin{bmatrix} v_{AN} \\ v_{BN} \\ v_{CN} \end{bmatrix} = \frac{E}{6} \begin{bmatrix} +2 & -1 & -1 \\ -1 & +2 & -1 \\ -1 & -1 & +2 \end{bmatrix} \begin{bmatrix} signe(ua - uo) \\ signe(ub - uo) \\ signe(uc - uo) \end{bmatrix} \quad (2)$$

In fact, the SVM technique allows direct control of the instantaneous values, enabling dynamic control of speed and current and the synthesis of high-performance controls for three-phase machines.

In addition, it improves the quality of the current delivered by the inverter, since harmonics are far from the fundamental [13].

This technique is based on the synthesis of the three control signals according to the desired voltage vector from the eight vectors that the inverter can deliver.

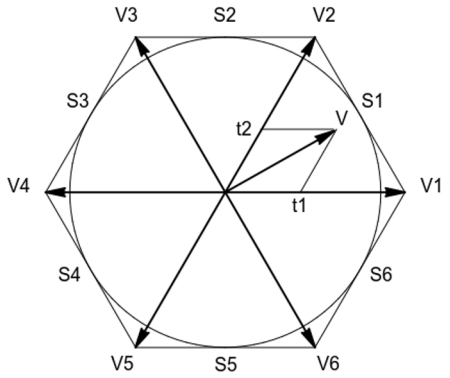

Fig. 1. SVM principle

The desired voltage vector located on one of the six sectors is a combination of the vectors delimiting this sector plus one of the two null vectors [14]. This is ensured by the intersection of the triangular carrier and the values of the reference signals previously calculated using equation (1).

$$\begin{bmatrix} ua \\ ub \\ uc \end{bmatrix} = [X] \begin{bmatrix} sin\frac{k\pi}{3} & -cos\frac{k\pi}{3} \\ -sin\frac{(k-1)\pi}{3} & cos\frac{(k-1)\pi}{3} \end{bmatrix} \begin{bmatrix} u\alpha \\ u\beta \end{bmatrix} \quad (3)$$

The matrix $[X]$ given in Table. 1 depends on the sector $\boldsymbol{k}$.

Table. 1. Reference generation of SVM

$\boldsymbol{k}$	1	2	3	4	5	6
$[X]$	$\begin{bmatrix} +1 & +1 \\ -1 & +1 \\ -1 & -1 \end{bmatrix}$	$\begin{bmatrix} +1 & -1 \\ +1 & +1 \\ -1 & -1 \end{bmatrix}$	$\begin{bmatrix} -1 & -1 \\ +1 & +1 \\ -1 & +1 \end{bmatrix}$	$\begin{bmatrix} -1 & -1 \\ +1 & -1 \\ +1 & +1 \end{bmatrix}$	$\begin{bmatrix} -1 & +1 \\ -1 & -1 \\ +1 & +1 \end{bmatrix}$	$\begin{bmatrix} +1 & +1 \\ -1 & -1 \\ +1 & -1 \end{bmatrix}$

4 Simplification of the $PMSM$ model in the rotor reference frame

In the two-phase rotor reference frame, the electromagnetic state space representation of the three-phase synchronous motor has two state space variables: direct and quadrature currents [15][16].

The control variables are the two voltages: direct and quadrature. Its matrix expression is recalled in equation (4) and completed by the mechanical equation (5).

$$\frac{d}{dt}\begin{bmatrix} i_d \\ i_q \end{bmatrix} = \begin{bmatrix} -\frac{1}{Td} i_d + p\Omega \frac{L_q}{L_d} i_q \\ -\frac{1}{Tq} i_q - p\Omega \frac{L_d}{L_q} i_d - p\Omega \varphi_M \frac{1}{L_q} \end{bmatrix} + \begin{bmatrix} \frac{1}{L_d} & 0 \\ 0 & \frac{1}{L_q} \end{bmatrix} \begin{bmatrix} v_d \\ v_q \end{bmatrix} \quad (4)$$

$$\frac{d\Omega}{dt} = -\frac{1}{Tm}\Omega + \frac{3p}{2J}\left(\varphi_M i_q + \left(L_d - L_q\right) i_d i_q\right) - \frac{C_R}{J} \quad (5)$$

First, we write the electromagnetic equation of state (6) for currents in vector form for greater clarity.

$$\dot{X}_i = F_i + G_i U \quad (6)$$

In this equation we define:

$$X_i = \begin{bmatrix} i_d \\ i_q \end{bmatrix} \quad (7)$$

$$F_i = \begin{bmatrix} -\frac{1}{Td} i_d + p\Omega \frac{L_q}{L_d} i_q \\ -\frac{1}{Tq} i_q - p\Omega \frac{L_d}{L_q} i_d - p\Omega \varphi_M \frac{1}{L_q} \end{bmatrix} \quad (8)$$

$$G_i = \begin{bmatrix} \frac{1}{L_d} & 0 \\ 0 & \frac{1}{L_q} \end{bmatrix} \quad (9)$$

$$U = \begin{bmatrix} v_d \\ v_q \end{bmatrix} \quad (10)$$

Furthermore, we assume that the fast variables, which are the currents, have reached their reference values when it comes to tackling the speed loop, which is the slow variable in this synthesis [17].

$$i_d = i_{dref} = 0 \;\; ; \;\; i_q = i_{qref} \neq 0 \quad (11)$$

Thus, the mechanical equation (5) is simplified as given in equation (12).

$$\frac{d\Omega}{dt} = -\frac{1}{Tm}\Omega + \frac{3p}{2J}\varphi_M i_{qref} - \frac{C_R}{J} \quad (12)$$

5 Design of Backstepping control strategy for a PMSM

5.1 $Backstepping$ control for the $PMSM$

We develop a two-stage design. The first stage is devoted to controlling the speed variable, which generates the quadrature current reference signal, and the second to controlling the currents [4][18].

5.1.1 First stage :

We define the velocity error and express its derivative by introducing a stabilizing term.

$$e_\Omega = \Omega - \Omega_{ref} \quad (13)$$

$$\dot{e}_\Omega = -\frac{1}{Tm}\Omega + \frac{3p}{2J}\varphi_M i_{qref} - \frac{C_R}{J} - \dot{\Omega}_{ref} = -k_\Omega e_\Omega \mid k_\Omega > 0 \quad (14)$$

The following $Lyapunov$ candidate function proves the stability of the control adopted in this step.

$$V_\Omega = \frac{1}{2}e_\Omega^2 > 0 \rightarrow \dot{V}_\Omega = e_\Omega \dot{e}_\Omega = -k_\Omega e_\Omega^2 < 0 \quad (15)$$

Finally, we express the control law that generates the quadrature current reference and calculate the control algorithm parameter from the response time [3].

$$i_{qref} = \left(\frac{3p}{2J}\varphi_M\right)^{-1}\left(-k_\Omega e_\Omega + \frac{1}{Tm}\Omega + \frac{C_R}{J} + \dot{\Omega}_{ref}\right) \quad (16)$$

5.1.2 Second stage :

We now need to control the currents using fast loops, taking into account the quadrature current reference from the slow loop in the first part, as well as a zero reference for the direct current, in order to simplify the expression of the electromagnetic torque and minimize the current absorbed by the motor [19].

We define the current error, express its derivative and introduce the stabilizing term.

$$E_i = X_i - X_{iref} = \begin{bmatrix} i_d \\ i_q \end{bmatrix} - \begin{bmatrix} i_{dref} \\ i_{qref} \end{bmatrix} = \begin{bmatrix} i_d \\ i_q \end{bmatrix} - \begin{bmatrix} 0 \\ i_{qref} \end{bmatrix} \quad (17)$$

$$\dot{E}_i = \dot{X}_i - \dot{X}_{iref} = F_i + G_i U - \dot{X}_{iref} = -K_{dq}E_i \quad (18)$$

With:

$$K_{dq} = \begin{bmatrix} k_d & 0 \\ 0 & k_q \end{bmatrix} \quad (19)$$

In fact, the following $Lyapunov$ candidate function justifies the stability of the direct and quadrature current loops.

$$V_i = \frac{1}{2}E_i^T E_i > 0 \rightarrow \dot{V}_i = E_i^T \dot{E}_i = -E_i^T K_{dq} E_i < 0 \mid K_{dq} > 0 \quad (20)$$

The final control law contains the expressions of the two parts of the synthesis.

$$\dot{E}_i = F_i + G_i U - \dot{X}_{iref} = -K_{dq}E_i \quad (21)$$

$$U = G_i^{-1}(-K_{dq}E_i - F_i + \dot{X}_{iref}) \quad (22)$$

5.2 Proposed method for calculating *PMSM* controller parameters using Backstepping Strategy

The controller parameters are calculated from the speed response time $trv = 100\ ms$, and the current response time $tri = 10\ ms$.

These values were chosen to ensure dynamic separation the one hand, and to limit the current draw during the transient regime on the other [4].

From equations (14) and (18), we express the equations of state for the errors (23) relating to the motor speed and its currents: direct and quadrature.

$$\dot{e}_\Omega = -k_\Omega e_\Omega \ ; \ \dot{E}_i = \begin{bmatrix} -k_d & 0 \\ 0 & -k_q \end{bmatrix} E_i \quad (23)$$

Equation (23) is the combination of three linear first orders, whose relationship between response time and time constant is used to determine the controller parameters.

$$trv = \frac{3}{k_\Omega} \rightarrow k_\Omega = \frac{3}{trv} = 30 \quad (24)$$

$$tri = \frac{3}{k_d} = \frac{3}{k_q} \rightarrow k_d = k_q = \frac{3}{tri} = 300 \quad (25)$$

6 Load torque observer

The $Backstepping$ strategy does not allow for disturbance rejection, especially when it is not equipped with integrators. A load torque observer is therefore required.

A $Luenberger$ observer is adopted to integrate de load torque value in the control law [3][4].

We express speed and load torque in the state-space form, neglecting the effect of direct current:

$$\frac{d}{dt}\begin{bmatrix} \Omega \\ C_R \end{bmatrix} = \begin{bmatrix} -\frac{1}{Tm} & -\frac{1}{J} \\ 0 & 0 \end{bmatrix}\begin{bmatrix} \Omega \\ C_R \end{bmatrix} + \begin{bmatrix} \frac{3p}{2J}\varphi_M \\ 0 \end{bmatrix} i_q \quad (26)$$

So the observer is driven by quadrature current and velocity. This is expressed in equation (27).

$$\frac{d}{dt}\begin{bmatrix} \tilde{\Omega} \\ \tilde{C}_R \end{bmatrix} = \begin{bmatrix} -\frac{1}{Tm} & -\frac{1}{J} \\ 0 & 0 \end{bmatrix}\begin{bmatrix} \tilde{\Omega} \\ \tilde{C}_R \end{bmatrix} + \begin{bmatrix} \frac{3p}{2J}\varphi_M \\ 0 \end{bmatrix} i_q - \begin{bmatrix} k_1 \\ k_2 \end{bmatrix}(\tilde{\Omega} - \Omega) \quad (27)$$

To determine the observer parameters, we establish the state space equation of the observation errors [20].

$$\frac{d}{dt}\begin{bmatrix} \tilde{\Omega} - \Omega \\ \tilde{C}_R - C_R \end{bmatrix} = \begin{bmatrix} -\frac{1}{Tm} - k_1 & -\frac{1}{J} \\ -k_2 & 0 \end{bmatrix}\begin{bmatrix} \tilde{\Omega} - \Omega \\ \tilde{C}_R - C_R \end{bmatrix} \quad (28)$$

So let's proceed with pole placement by identification with a suitably chosen characteristic polynomial.

$$det\begin{bmatrix} \lambda + \frac{1}{Tm} + k_1 & \frac{1}{J} \\ k_2 & \lambda \end{bmatrix} = \lambda^2 + \left(\frac{1}{Tm} + k_1\right)\lambda - \frac{k_2}{J}$$

$$= \lambda^2 + 2m\omega_n\lambda + \omega_n^2 \quad (29)$$

$$m = 1 \rightarrow \omega_n = \frac{4.75}{tro} = \frac{4.75}{0.010} = 475 \quad (30)$$

$$k_1 = 2\omega_n - \frac{1}{Tm} = 950 \ ; \ k_2 = -J\omega_n^2 = -2256 \quad (31)$$

7 Validation of the proposed controller using *PIL* technique

The SVM modulator period and calculation step were set to 100 μs during this test.

The implementation scheme on $Simulink$ shown in Fig. 3 allows the generation of the code for the control algorithm and ensures validation by the PIL technique [21][22].

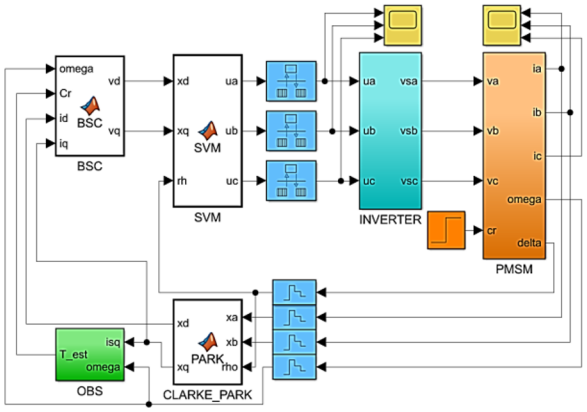

Fig. 2. Simulink implementation of Backstepping control strategy for PMSM drive

The results of this experiment are shown in figures Fig. 4 to Fig. 7.

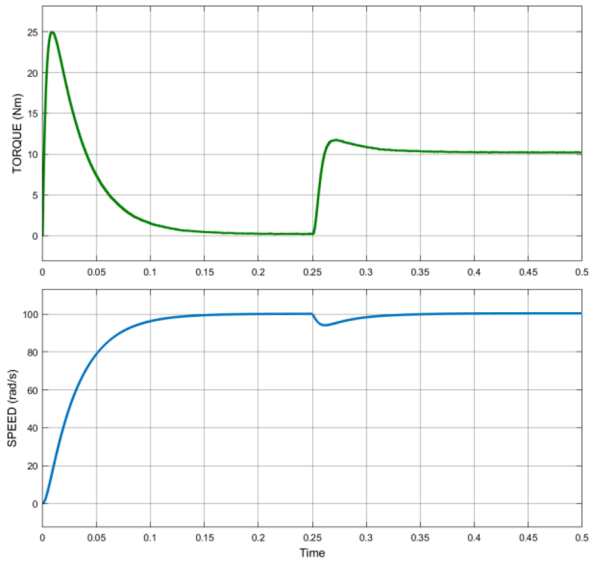

Fig. 3. Torque and spped of the PMSM controlled using Backstepping strategy

We found that the obtained speed response time value $trv \approx 100\,ms$, and accuracy met the requirements, and that the torque was smooth. We can enhance the disturbance rejection by decreasing the response time of the load torque observer.

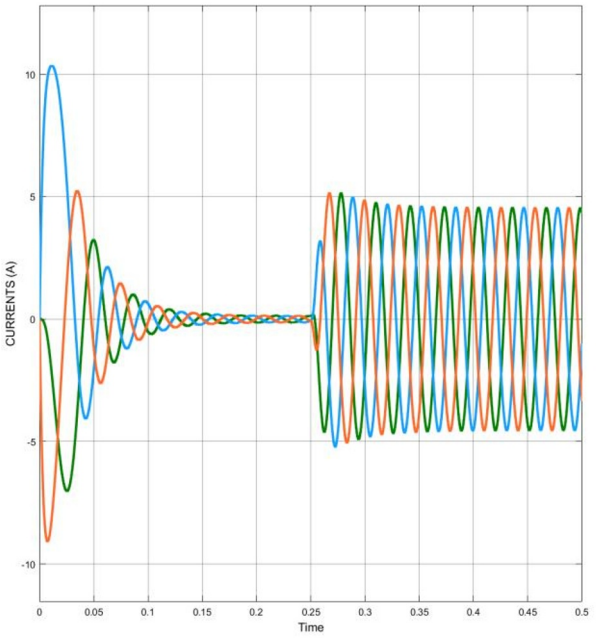

Fig. 4. Curents absorbed by the PMSM in Backstepping contro strategy

Current distortion is not perceptible because of the short SVM period 100 μs. The start-up peak is acceptable. We notice also that the current on no load regime is low for $PMSM$.

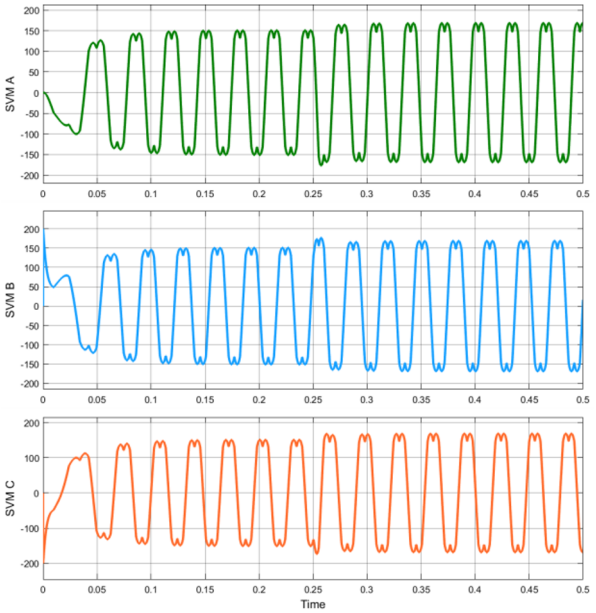

Fig. 5. The SVM signals driving the inverter during Backstepping control of the PMSM

SVM signals are undistorted. The deformation in the middle is due to the load torque step.

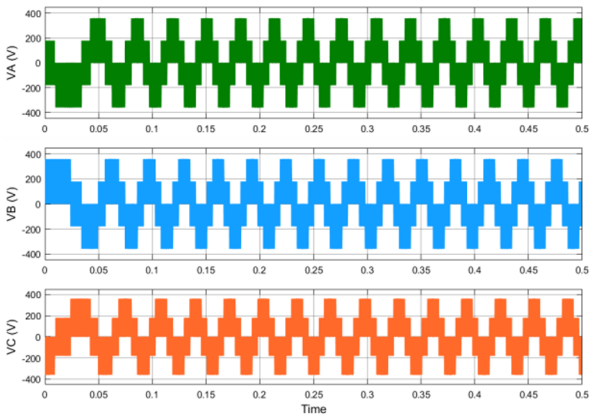

Fig. 6. Stator voltages generated by the SVM inverter during the PMSM Backstepping control

The supply voltages from the SVM inverter are highly distorted and contain high-frequency harmonics. These harmonics are filtered out by the motor inductances, and are therefore attenuated in the absorbed currents by the machine itself, which acts as a low-pass filter.

8 Conclusion

$Backstepping$ control is an advanced nonlinear control strategy that can be easily adapted to nonlinear $SISO$ or $MIMO$ systems such as AC motors. The design of this control law begins by modeling the motor in the appropriate two-phase reference frame, in order to obtain simpler equations. We proposed expressing the mathematical model of synchronous motor in vector form.

Then, we proposed a Backstepping control design that is performed in two steps imposed by the order of the motor model. Furthermore, in order to minimize the effect of load torque on speed, we proposed to introduce a load torque observer which is synthesized according to the $Luenburger$ method. We have also added integral actions for greater accuracy.

This paper also proposed, following our design, the development of a systematic method for calculating controller parameters by $Backstepping$ from specifications such as response time, accuracy and damping coefficient.

We proposed designing this control by separating the slow variable which is the speed of the $PMSM$ from the fast variables which are the currents. In the case of the MSAP, there was no need to estimate the flux generated by the permanent magnets, as it is constant.

We implemented a cosimulation validation platform based on the $LAUNCHXL - F28069M$ development board, $Matlab|Simulink$ software and the $Code\ Compose\ Studio$ integrated development environment. We carried out the first tests on $Simulink$, from which the codes for the control algorithms are generated, and then validated them on the $Texas\ Instruments\ F28069M$ board using the $Processor\ In\ the\ Loop$: PIL technique. In this way, the code runs on a DSP and communicates with the motor model powered by an SVM inverter on $Simulink$ via USB in a serial link.

We can improve speed control using a faster load torque observer. Robustness may be enhanced using an adaptive $Backstepping$ strategy.

Table. 2. System numerical specifications

Rated output power :	$1500\ W$
Rated load torque :	$10\ Nm$
Rated speed :	$1500\ rpm; p = 2$
Rated voltage | frequency :	$220/380V; 50\ Hz$
Resistance :	$Rs\ = 2.5\ \Omega$
Direct inductance :	$Ld\ = 25\ mH$
Quadratic inductance :	$Lq\ = 75\ mH$
Moment of inertia :	$J = \ 0.01\ kg.m^2$
Coefficient of friction :	$f = 0.002\ Nm/rad.s^{-1}$
Time constants :	$Td\ = 10\ ms;\ Tq\ = 30\ ms$
Mechanic time constant :	$Tm = 5\ s$
DC bus voltage :	$E\ = 220\sqrt{2}\sqrt{3} = 539\ V$

Table. 3. Nomenclature

Ω	Rotor speed
C_R	Load torque
v_d, v_q	Direct and quadratic stator voltages
i_d, i_q	Direct and quadratic stator currents
PIL	Processor In the Loop
CCS	Code Composer Studio
$PMSM$	Permanent Magnet Synchronous Motor
SVM	Space Vector Modulation
R_S	Stator resistance
$L_d,\ L_q$	Direct and quadratic inductances
J, f	Inertia and coefficient of friction
Td, Tq	Direct and Quadratic time constants
p	Number of pole pairs
φ_M	Permanent magnet flux linkage

References

[1] S. Rudra, R. K. Barai, and M. Maitra, *Block Backstepping Design of Nonlinear State Feedback Control Law for Underactuated Mechanical Systems*. Editions Springer, 2017.

[2] T. Meurer, *Control of Higher-Dimentional PDEs, Flatness and Backstepping Design*. Editions Springer, 2013.

[3] M. El Haissouf, M. El Haroussi, and A. Ba-Razzouk, "Processor in the Loop Experimentation of an Integral Backstepping Control Strategy Based Torque Observer for Induction Motor Drive," *Int. Rev. Autom. Control*, vol. 16, no. 2, pp. 92–103, 2023, doi: 10.15866/ireaco.v16i2.23063.

[4] M. El haissouf, M. Elharoussi, and A. Ba-razzouk, "Backstepping control strategy for induction motor with rotor flux and load torque observers," *ITM Web Conf.*, vol. 48, p. 04002, 2022, doi: 10.1051/itmconf/20224804002.

[5] J. Kabzinski, *Advanced Control of Electrical Drives and Power Electronic Converters*. Editions Springer, 2017.

[6] S. Massoum, A. Meroufel, A. Massoum, W. Patrice, and A. Massoum, "DTC based on SVM for induction motor sensorless drive with fuzzy

sliding mode speed controller," *IJECE*, vol. 11, no. 1, pp. 171–181, 2021, doi: 10.11591/ijece.v11i1.pp171-181.

[7] M. El Haissouf, M. El Haroussi, and A. Ba-Razzouk, "DSP In the Loop implementation of an improved sliding mode control for induction motor drive," *IJPEDS*, 2023, doi: 10.11591/ijpeds.v15.i1.pp53-63.

[8] M. El Haissouf, M. El Haroussi, and A. Barazzouk, "DSP In the Loop Implementation of an Enhanced Sliding Mode Control for Permanent Magnet Synchronous Motor," *IREE*, 2023, doi: 10.15866/iree.v18i4.23399 .

[9] E. Lotfi, B. Rached, M. Elhaissouf, M. Elharoussi, and E. Abdelmounim, "DSP implementation in the loop of the vector control drive of a permanent magnet synchronous machine," in *ACM International Conference Proceeding Series*, 2017, pp. 1–7, doi: 10.1145/3167486.3167542.

[10] N. Murali, "Modified V-Shaped Interior Permanent Magnet Synchronous Motor Drives for Electric Vehicles," *IREMOS*, vol. 14, no. December, 2021.

[11] A. Moualdia, A. Medjber, A. Kouzou, and O. Bouchhida, "DTC-SVPWM of an energy storage flywheel associated with a wind turbine based on the DFIM," *Sci. Iran.*, vol. 25, pp. 3532–3541, 2018, doi: 10.24200/sci.2017.4379.

[12] V. R. Reddy and V. C. V. Reddy, "Mathematical Analysis of SVPWM for Inverter fed DTC of Induction motor Drive," *Int. J. Appl. Eng. Res.*, vol. 13, no. 1, pp. 47–52, 2018.

[13] G. Satheesh, T. B. Reddy, and C. H. S. Babu, "SVPWM Based DTC of OEWIM Drive Fed With Four Level Inverter with Asymmetrical DC Link Voltages," *IJSCE*, vol. 2, no. 1, pp. 64–68, 2013.

[14] C. H. Krishna, J. Amarnath, and S. Kamakshiah, "A Simplified SVPWM Algorithm for Multi-Level Inverter fed DTC of Induction Motor Drive," *IJEIT*, vol. 1, no. 4, pp. 61–67, 2012.

[15] J. Wang, Q. Miao, X. Zhou, L. Sun, D. Gao, and H. Lu, "Current Control Method of Vehicle Permanent Magnet Synchronous Motor Based on Active Disturbance Rejection Control," *World Electr. Veh. J.*, 2023.

[16] H. Ghanayem and M. Alathamneh, "Decoupled Speed and Flux Control of Three-Phase PMSM Based on the Proportional-Resonant Control Method," *energies*, 2023.

[17] S. D. Kumar and A. Jagadeeshwaran, "A Sensor-less Surface Mounted PMSM for Electronic Speed Control in Multilevel Inverter," *Intell. Autom. Soft Comput.*, 2023, doi: 10.32604/iasc.2023.027467.

[18] G. Prior and M. Krstic, "Quantized-Input Control Lyapunov Approach for Permanent Magnet Synchronous Motor Drives," *IEEE Trans. Control Technol.*, vol. 21, no. 5, pp. 1784–1794, 2013.

[19] D. Karboua, B. Toual, A. Kouzou, B. O. Douara, T. Mebkhouta, and A. N. Bendenidina, "High-order Supper-twisting Based Terminal Sliding Mode Control Applied on Three Phases Permanent Synchronous Machine," *Period. Polytech. Electr. Eng. Comput. Sci.*, vol. 67, no. 1, pp. 40–50, 2023.

[20] C. Chen, H. Yu, F. Gong, and H. Wu, "Induction Motor Adaptive Backstepping Control and Efficiency Optimization Based on Load Observer," *energies*, 2020, doi: 10.3390/en13143712.

[21] M. Elhaissouf, E. Lotfi, B. Rached, M. Elharoussi, and A. Barazzouk, "DSP implementation in the loop of the indirect rotor field orientation control for the three-phase asynchronous machine," in *ACM International Conference Proceeding Series*, 2017, no. 1, pp. 1–7, doi: 10.1145/3167486.3167541.

[22] S. Motahhir, A. El Ghzizal, S. Sebti, and A. Derouich, "MIL and SIL and PIL tests for MPPT algorithm," *Cogent Eng.*, vol. 98, no. March 2020, 2017, doi: 10.1080/23311916.2017.1378475.